

1 Conference Proceedings Paper

2 **Hirshfeld surface analysis and energy framework for**
3 **crystals of quinazoline methyldiene bridged**
4 **compounds**

5 **Akmaljon Tojiboev** ^{1,*}, **Sherzod Zhurakulov** ^{2,4}, **Ulli Englert** ³, **Ruimin Wang** ³, **Irmgard Kalf** ³,
6 **Valentina Vinogradova** ², **Kambarali Turgunov** ^{2,5} and **Bakhodir Tashkhodjaev** ²

7 ¹ Arifov Institute of Ion-Plasma and Laser Technologies of Uzbekistan Academy of, Sciences, 100125, Durmon
8 yuli st. 33, Tashkent, Uzbekistan; info@iplt.uz

9 ² S.Yunusov Institute of Chemistry of Plant Substances, Academy of Sciences of Uzbekistan, Mirzo Ulugbek
10 Str. 77, 100170 Tashkent, Uzbekistan; ; cnc@icps.org.uz

11 ³ Institute of Inorganic Chemistry, RWTH Aachen University, Landoltweg 1, 52056, Aachen, Germany;
12 ullrich.englert@ac.rwth-aachen.de

13 ⁴ National University of Uzbekistan named after Mirzo Ulugbek, 100174 University str 4 Olmazor district
14 Tashkent, Uzbekistan; devonxona@nuu.uz

15 ⁵ Turin Polytechnic University in Tashkent, Kichik Khalka yuli str., 17, 100095 Tashkent, Uzbekistan;
16 info@polito.uz

17 * Correspondence: a_tojiboev@yahoo.com

18 Published: 20 November 2020

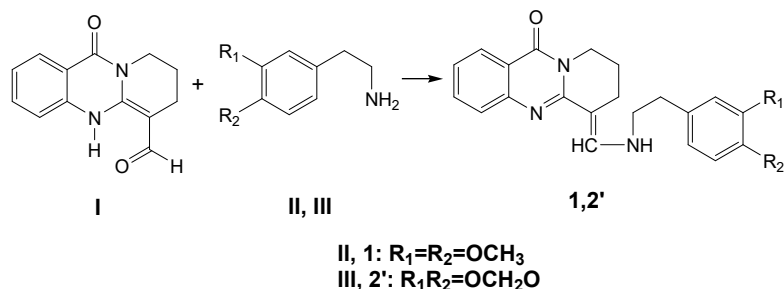
19
20 **Abstract:** The crystal structures of 4-(3,4-dimethoxyphenylethylamino)-
21 methyldiene-2,3,4,10-tetrahydro-1H-pyrido[2,1-b]-quinazolin-10-one (1) and 4-(3,4-
22 methylenedioxyphenylethylamino)-methyldiene-2,3,4,10-tetrahydro-1H-pyrido[2,1-b]-quinazolin-
23 10-one hydrochloride (2) were studied by single crystal X-ray diffraction. Their molecular and
24 crystal structures are described in the context of intra- and inter-molecular interactions and of
25 stereoisomerism. The crystallographic study established mixed *E*, *Z* configuration about the
26 C4=C12 bond for (1) and *E* configuration about the C4=C12 bond for (2). For molecular crystals,
27 Hirshfeld surface analyses may provide insight into intermolecular interactions, and energy
28 framework analyses allow to quantify different contributions to the overall energy. These analyses
29 were performed to pinpoint intermolecular interactions in (1) and (2). According to our results, the
30 molecules are associated by intra- and intermolecular hydrogen bonds, C–H··· π and π -stacking
31 interactions. The three-dimensional Hirshfeld surface analyses and two-dimensional fingerprint
32 plots revealed that the structures are dominated by H···H, H···C/C···H and H···O/O···H contacts.
33 The intermolecular energy analysis confirmed a significant contribution of dispersion to the
34 stabilization of molecular packings in (1) and (2).

35 **Keywords:** crystal structure; quinazoline; intermolecular interaction energy.
36

37 **1. Introduction**

38 Quinazoline alkaloids are heterocycles containing tricyclic rings and represent an interesting
39 group among alkaloids found in plants of the genus *Peganum*, *Adhatoda*, *Galega*, *Galium*, *Nitraria*, etc.
40 [1,2]. Alkaloids with biological activity and use in medical practice have been found in this series.
41 Among them, deoxypeganine and deoxyvazicinone, isolated from the plant *Peganum harmala* have
42 a particular interest. Deoxypeganine is an anticholinesterase drug in form of the deoxypeganine

43 hydrochloride [3,4]. Deoxyvazicinone shows antimicrobial and anti-inflammatory activity [5, 6]. The
 44 alkaloid makinazolinone was first isolated from the plant *Mackilaya subulata* Philipson [7]. In order
 45 to identify factors relevant for the reactivity of 4-(formyl)-2,3,4,10-tetrahydro-1H-pyrido[2,1-b]-
 46 quinazoline-10-one (**I**) towards nucleophilic substitution, we carried out the amination reaction
 47 4-(formyl)-2,3,4,10-tetrahydro-1H-pyrido[2,1-b]-quinazoline-10-one (**I**) c 3,4- dimethoxyphenyl-
 48 ethylamine (**II**) and 3,4-methylenedioxyphenylethylamine (**III**) according to a published method
 49 [8-12] and obtained the derivatives (1) and (2). These studies continue our research in this direction
 50 [13]. A reaction scheme for the synthesis of the title compounds is illustrated in Scheme I. In this
 51 contribution, we describe the molecular and crystal structures of the target compounds and perform
 52 a Hirshfeld surface analysis to visualize intermolecular interactions.
 53



54 **Scheme I.** Reaction scheme.

55

56 2. Materials and Methods

57 2.1. General Experiment and Synthesis

58 A detailed report on the synthesis of (1), (2) and its characterization by IR, ¹H NMR is available
 59 in [14-16]. Synthesis of 4-(3,4-methylenedioxyphenylethylamino)-methylidene-2,3,4,10-tetrahydro-
 60 1H-pyrido[2,1-b]-quinazolin-10-one hydrochloride (2): 4-(3,4-methylenedioxyphenylethylamino)-
 61 methylidene-2,3,4,10-tetrahydro-1H-pyrido[2,1-b]-quinazolin-10-one (2') was dissolved in acetone
 62 and acidified with concentrated HCl to pH 5-6. The precipitated hydrochloride was separated by
 63 filtration and recrystallized from methanol. Crystals suitable for X-ray diffraction were obtained
 64 from a solution in methanol by slow evaporation of the solvent at room temperature.

65 2.2. Crystallographic Details

66 Crystal diffraction data were collected: for (1) on the EH1 Kappa diffractometer equipped with
 67 a Dectris CdTe area detector using synchrotron radiation at beamline P24, DESY, Hamburg and for
 68 (2) on a Bruker D8 diffractometer equipped with an APEX CCD detector and multilayer optics
 69 microfocus tube with MoK α radiation. The crystals of (1) were extremely small because of this it was
 70 used synchrotron radiation. Absorption correction was not applied for (1). Crystal structures of (1)
 71 and (2) were solved by direct methods with the program SHELXS [17] and refined by full-matrix
 72 least-squares on F^2 with the SHELXL [18] package.

73 In the crystal structure (1), H atoms attached to C were positioned geometrically and treated as
 74 riding on their parent atoms, with C–H = 0.95 (aromatic), 0.98 (methyl), 0.99 (methylene) Å and
 75 were refined with $U_{iso}(H) = 1.5U_{eq}(C)$ for methyl H atoms and $1.2U_{eq}(C)$ otherwise. The H atom in the
 76 enamine group was refined with a distance restraint [target distance N–H = 0.95 Å] and with
 77 $U_{iso}(H) = 1.2U_{eq}(N)$. The residual density is high (0.85 e Å⁻³) due to the extensive disorder.

78 In the crystal structure of (2), H atoms attached to C were positioned geometrically and treated
 79 as riding on their parent atoms, with C–H = 0.95 (aromatic), 0.99 (methylene) Å and were refined
 80 with $1.2U_{eq}(C)$ otherwise. The H atom bonded to nitrogen was constrained with a distance 0.88 Å
 81 and with $U_{iso}(H) = 1.2U_{eq}(N)$.

82 Details of the crystallographic data collection, structural determination and refinement for (1)
 83 and (2) are summarized in Table S1(See Supplementary Materials). Full data set is available in form
 84 of CIF files, deposited with the CCDC (2039173, 2039174), and may be obtained free of charge via
 85 <https://www.ccdc.cam.ac.uk/structures>.

86 2.3. Hirshfeld Surface Calculations

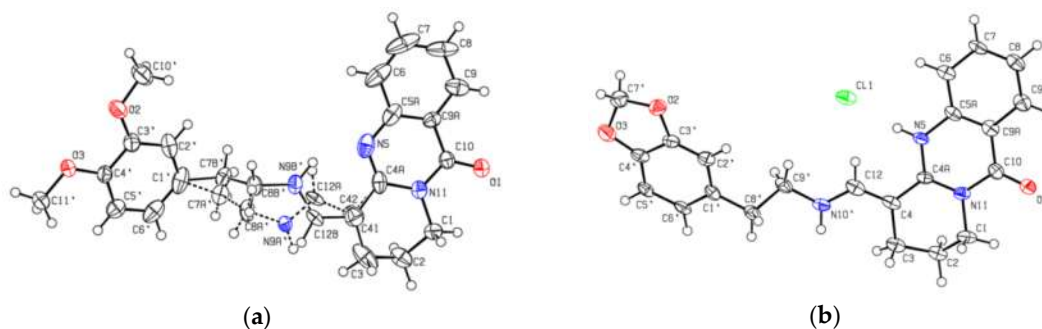
87 The Hirshfeld surface (HS) is the area around a molecule in crystal space which separates two
 88 regions, that of the inner reference molecule from the outer neighboring molecules. The separation
 89 of space by the HS allows the analysis of intermolecular interactions of fingerprints in a crystalline
 90 medium [19, 20]. HS analysis can be employed to visualize and quantify various non-covalent
 91 interactions that stabilize the crystal packing. HS can be mapped with different properties, namely
 92 d_{norm} , electrostatic potential, shape index and curvature. The d_{norm} property is a symmetric function
 93 of distances to the surface between nuclei inside and outside the Hirshfeld surface (d_i and d_e ,
 94 respectively), relative to their respective van der Waals radii. The regions with red and blue color on
 95 the d_{norm} represent the shorter and longer inter contacts while the white color indicates the contacts
 96 around the van der Waals radii. 2D fingerprint plots provide relevant information of intermolecular
 97 contacts in the crystal. The HS analysis has become a very useful tool for explaining the nature of
 98 intermolecular interactions that affect the packing of molecules in crystals [21]. Hirshfeld surfaces
 99 analysis are widely used to study the phenomena of polymorphism [22, 23], co-crystallization [24],
 100 the inclusion of small molecules in the cavities of macromolecules [25, 26], and the search for
 101 correlations between the strength of interactions and the melting point [27].

102 The HS analyses and their associated 2D fingerprint plots (full and decomposed) [28] were
 103 carried out employing the *CrystalExplorer* 17.5 program [29]. The d_{norm} surface was mapped with the
 104 color scale in the range -0.050 au (red) to 0.600 au (blue). 2D fingerprint plots (d_i vs. d_e) were
 105 displayed using the expanded 0.6–2.8 Å range.

106 3. Results and Discussion

107 3.1. Structural Description

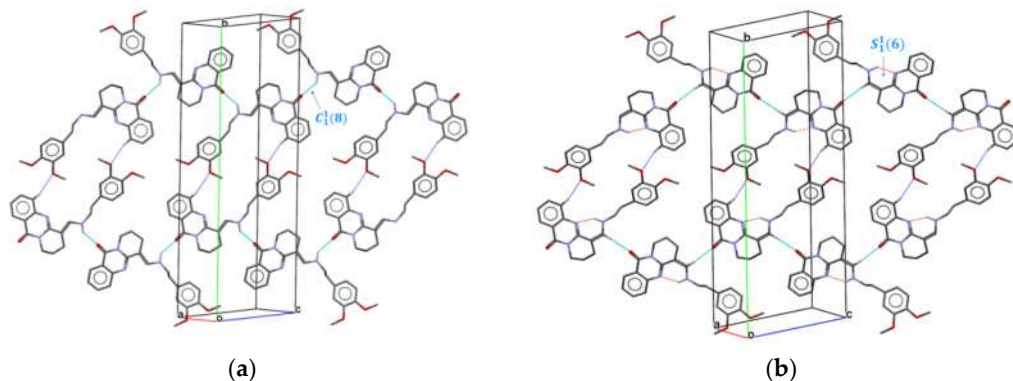
108 The compounds (1) and (2) crystallize in the monoclinic system in space group $P2_1/c$.
 109 Displacement ellipsoid plots and numbering schemes for both molecules are provided in Figure 1.
 110



111 **Figure 1.** Displacement ellipsoid plot [33] of the asymmetric unit of: (a)
 112 4-(3,4-dimethoxyphenylethylamino)-methylidene-2,3,4,10-tetrahydro-1H-pyrido[2,1-b]-quinazolin-
 113 10-one (1) ; (b) of 4-(3,4-methylenedioxyphenylethylamino)-methylidene-2,3,4,10-tetrahydro-1H-
 114 pyrido[2,1-b]-quinazolin-10-one hydrochloride (2) and atom-labeling scheme. Ellipsoids are drawn
 115 at 50% probability; H atoms are shown as spheres of arbitrary radius.

116 For the structure of (1), X-ray diffraction revealed that the binding enamine group is disordered,
 117 leading to the formation of *E* and *Z* isomers about the C4=C12 double bond. In case of the *E*
 118 configuration, an O··H–N intermolecular hydrogen bond links the N atom of the enamine group to
 119 the keto group of the quinazoline moiety and gives rise to an $C_1^1(8)$ chain motif connecting adjacent

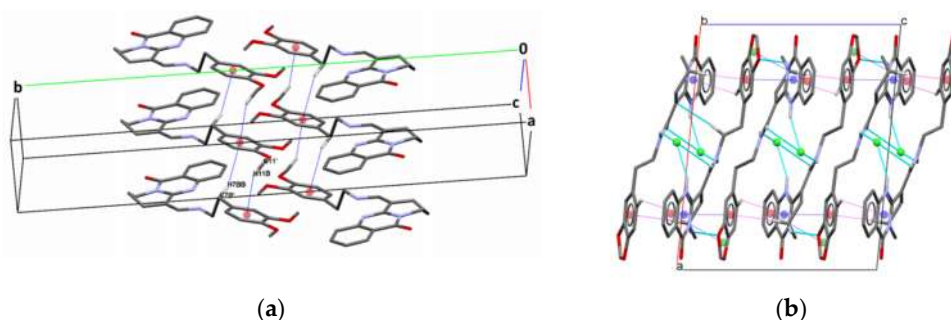
120 molecules to zigzag like chains propagating along the *b*-axis (Figure 2a). In case of the *Z*
 121 configuration an N9B'-H9B'...N5 intramolecular hydrogen bond (2.812(8) Å) is formed, which
 122 generates an $S_1^1(6)$ ring motif (Figure 2b). In both cases an additional C6-H6...O2 hydrogen bond
 123 leads to a two-dimensional network parallel to (102) plane (Figure 2a,b and Figure S1). The
 124 hydrogen-bond geometry for (1) is listed in Table S2.
 125



126 **Figure 2.** Packing for the alternative configurations of (1) along the *b*-axis, showing interactions in the
 127 layers. C—H...O hydrogen bonds as dark blue dashed lines; (a) O...H—N intermolecular hydrogen
 128 bonds are represented as light-blue dashed lines, which generate $C_1^1(8)$ ring motif forming *E*
 129 configuration; (b) N—H...N intramolecular hydrogen bonds as red dashed lines, which generate $S_1^1(6)$
 130 ring motif forming *Z* configuration. H atoms not involved in hydrogen bonds have been omitted for
 131 clarity.

132 Figure 3a shows the interaction between adjacent molecules along the crystallographic *a*-axis. Cg_4
 133 denotes the centroid of the 3,4-dimethoxyphenylethylamino ring (C1'-C6'). In the *Z*-configuration of
 134 (1) both contacts C7B'—H7BB... Cg_4 and C11'—H11B... Cg_4 participate in the interaction between
 135 adjacent molecules, whereas in the case of the *E*-configuration only the latter contact contributes to
 136 C—H... π interactions.

137 Structure (2) consists of Cl⁻ counteranions and the organic cations. The latter are composed of
 138 tricyclic quinazoline and 3,4-methylenedioxyphenylethylamino units linked by an enamine group
 139 (Figure 1b). The crystallographic study of structure (2) revealed the *E* configuration about the
 140 C4=C12 double bond, similar to one of the alternative configurations in structure (1) (Figure 1b).
 141 N5—H5...Cl1 (3.088(5)Å) and N10'—10'...Cl1(3.187(6)Å) intermolecular hydrogen bonds links the Cl⁻
 142 anion to N atoms in the enamine group and the pyrimidine ring and give rise to a centrosymmetric
 143 dimer (Figure S2, Table S3) with $D_1^1(2)$, $R_4^2(16)$ graph motif. Additional short ring interactions
 144 $Cg_1—Cg_5$ (3.758(5)Å), $Cg_2—Cg_4$ (3.426(4)Å) and $Cg_4—Cg_5$ (3.662(4)Å) lead to formation of a three
 145 dimensional supramolecular network ($Cg_1(O1/C3'/C4'/O3/C7)$, $Cg_2(N5/C4A/N11/C10/C9A/C5A)$,
 146 $Cg_4(C1'-C6')$ and $Cg_5(C5A/C6-C9/C9A)$) (Figure 3b).
 147

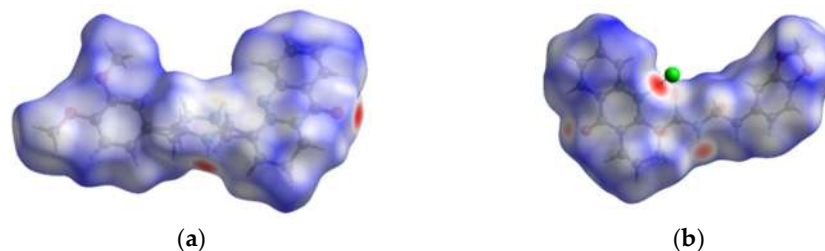


148 **Figure 3.** (a) C—H... π interactions between layers in the structure (1); (b) For structure (2) the
 149 packing diagram viewed along the *b*-axis with the interactions C—H...O, C—H...Cl, N—H...Cl
 150 shown as blue dashed lines, C—H... π (ring) and $\pi—\pi$ stacking interactions shown as magenta and

151 dark blue dashed lines. Ring centroids are as spheres: Cg1- green; Cg2- blue; Cg4 and Cg5 – red; In
 152 both (a) and (b) figures, H atoms not involved in hydrogen bonds have been omitted.

153 3.2. Hirshfeld Surface Analysis

154 The intermolecular interactions in (1) and (2) have been further investigated and visualized by
 155 HS analyses performed with *CrystalExplorer17.5* [29]. d_{norm} mapped on the HS (Figure 4a,b) shows
 156 short intermolecular contacts as red spots. They correspond to C–H···O contacts in (1) (Figure 5a)
 157 and C–H···O and N–H···Cl hydrogen bonds in (2) (Figure 5b).
 158



159 **Figure 4.** View of the three-dimensional Hirshfeld surface: (a) of (1) plotted over d_{norm} in the range –
 160 0.5234 to 1.2437 a.u.; (b) of (2) plotted over d_{norm} in the range –0.5144 to 1.2154.

161 The overall fingerprint plot for (1) and (2) is shown in Figures 5a and 5f, respectively, and those
 162 decomposed into H···H, H···C/C···H, H···O/O···H, H···N/N···H and Cl···H/H···Cl contacts are
 163 illustrated in Figures 5(b-e),(g-j) together with their relative contributions to the Hirshfeld surface.

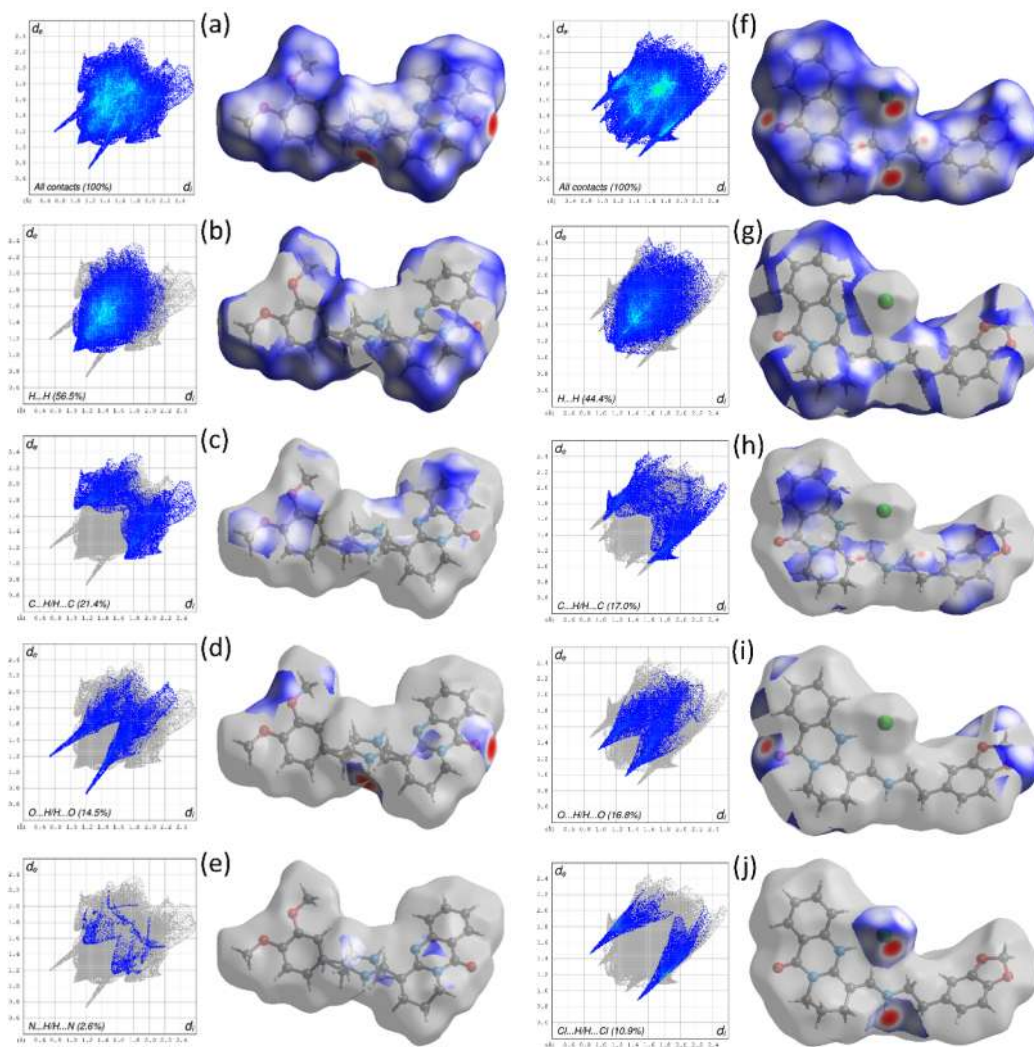
164 The most prominent type of contacts in (1) structure corresponds to H···H contacts; they
 165 contribute 56.5% to the overall surface contacts (Figure 5b). The presence of C–H··· π interactions
 166 gives rise to a pair of characteristic wings in the fingerprint plot decomposed into C···H/H···C
 167 contacts (Figure 5c) contributing 21.4% to the HS. Short O···H/H···O contacts (Figure 5d) contribute
 168 14.5% to the HS and form a pair of spikes. N···H/H···N contacts, contributing 2.6% to the overall
 169 surface, are depicted in Figure 5e as widely scattered wings.

170 For the structure (2) the fingerprint profile is dominated by H···H (44.4%) surface contacts
 171 (Figure 5g). C···H/H···C interactions contribute 17.0% of the total HS (Figure 5h) as pair wings.
 172 The pair of sharp spikes (Figure 5i) represents the H···O/O···H contacts with a contribution of 16.8%;
 173 they are due to intermolecular C–H···O hydrogen bonding. The fingerprint plot for Cl···H/H···Cl
 174 contacts (10.9% contribution) in Figure 5j, has a pair of spikes indicating C–H···Cl contacts.

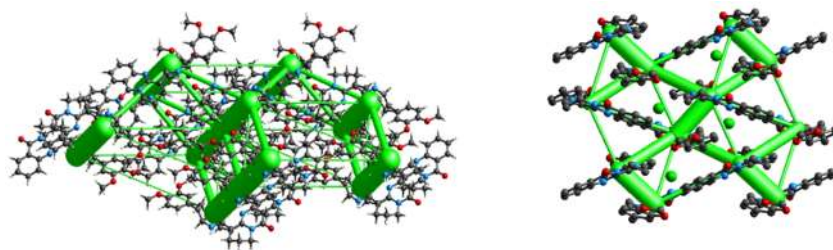
175 The contribution of other contacts to the Hirshfeld surface are negligible for both structures;
 176 they amount to H···N/N···H (2.6%), C···C (2.3%), C···N/N···C (1.8%), O···C/C···O (0.5%), N···N (0.3%)
 177 for (1) and to H···N/N···H (2.4%), C···N/N···C (1.7%), O···C/C···O (1.1%), O···O (0.4%), N···N (0.1%) for
 178 (2).

179 3.3. Interaction Energies

180 Interaction energies in (1) and (2) were calculated using CE-B3LYP/6-31G(d,p) quantum level of
 181 theory, as available in *CrystalExplorer*. The total intermolecular interaction energy (E_{tot}) is the sum of
 182 four energy terms: electrostatic (E_{ele}), polarization (E_{pol}), dispersion (E_{disp}) and exchange-repulsion
 183 (E_{rep}) with scale factors of 1.057, 0.740, 0.871 and 0.618, respectively. [31]. The relative strengths in
 184 interaction energies in individual directions are represented by cylinder-shaped energy frameworks
 185 (Figures 6). Insignificant contacts weaker than a threshold energy of 10 kcal/mol have been omitted
 186 from the original figure for clarity. Dispersion forces play the dominant role in (1) and (2) (Figure 6).
 187



188 **Figure 5.** Two-dimensional fingerprint plots for all intermolecular contacts in (1) (a) and (2) (f).
 189 Contributions of individual interactions: H...H for (1) (b) and (2) (g); C...H/H...C for (1) (c) and (2) (h);
 190 O...H/H...O for (1) (d) and (2) (i); N...H/H...C for (1) (e) and Cl...H/H...Cl for (2) (j). The outline of the
 191 full fingerprint plot is shown in grey. Surfaces to the right highlight the relevant d_{norm} surface patches
 192 associated with the specific contacts. The percentage of contribution is specified for each contact.



193 **Figure 6.** Energy-framework diagrams for E_{dis} for a cluster of molecules in (1) and (2). The cylindrical
 194 radius is proportional to the relative strength of the corresponding energy and was adjusted to the
 195 scale factor of 80 kJ mol^{-1} with a cut-off value of 10 kJ mol^{-1} .

196

197

198 4. Conclusions

199 A detailed structural analysis of 4-(3,4-dimethoxyphenylethylamino)-
200 methylidene-2,3,4,10-tetrahydro-1H-pyrido[2,1-b]-quinazolin-10-one (1) revealed disorder of the
201 enamine group, leading to the concomitant presence of *E* and *Z* isomers in the crystal. In the *E*
202 isomer an intermolecular N—H···O hydrogen bonds results in the formation of a $C_1^1(8)$ ring motif.
203 In the *Z* isomer an intramolecular N—H···N hydrogen bonds results in the formation of an $S_1^1(6)$
204 pattern.

205 The structure 4-(3,4-methylenedioxyphenylethylamino)-methylidene-2,3,4,10-tetrahydro-
206 1H-pyrido[2,1-b]-quinazolin-10-one hydrochloride (2) has the *E* configuration, similar to one of the
207 alternative configurations in structure (1). N—H···Cl intermolecular hydrogen bonds are forming a
208 centrosymmetric dimer with $D_1^1(2)$, $R_2^4(16)$ graph motifs.

209 The large number of H···H, H···C/C···H and H···O/O···H contacts revealed in (1) and (2) by a HS
210 analysis indicate that van der Waals interactions and hydrogen bonding mostly contribute to crystal
211 packing. Initial results on energy frameworks suggest that dispersion forces are relevant for the
212 topology of the overall interaction energies in these crystals of quinazoline derivatives.

213 **Supplementary Materials:** The following are available online at www.mdpi.com/xxx/s1, Figure S1: Layers are
214 propagating parallel to (102) plane. H atoms not involved in interactions have been omitted for clarity; Figure
215 S2: A partial packing diagram of the crystal of (2) with intramolecular C—H···O, C—H···N and intermolecular
216 C—H···O, C—H···Cl, N—H···Cl hydrogen bonds shown, respectively, by red and blue dashed lines. H atoms
217 not involved in hydrogen bonds have been omitted for clarity; Table S1: Crystal data and structure refinement
218 parameters for (1) and (2); Table S2: Hydrogen-bond geometry (Å, °) for (1). Cg4 is the centroids of ring (C1'–
219 C6'); Table S3: Hydrogen-bond geometry (Å, °) for (2). Cg2 and Cg4 are the centroids of ring
220 (N5/C4A/N11/C10/C9A/C5A) and (C1'–C6'), respectively.

221 **Author Contributions:** A.T., Sh.J., U.E. and K.T. conceived and designed the experiments, conceptualized the
222 work, and prepared the manuscript for publication; U.E. conducted the X-ray analysis, reviewed, and edited the
223 manuscript; U.E., R.W., B.T. and K.T. validated and formal analyzed; I.K. crystallization experiments; Sh.J. and
224 V.V. provided chemical synthesis; U.E. reviewed, and edited the manuscript. All authors have read and agreed
225 to the published version of the manuscript.

226 **Funding:** This work was supported by the Istedod Foundation of the Republic of Uzbekistan.

227 **Acknowledgments:** We thank Dr Carsten Paulmann for help with the synchrotron data collections and we are
228 grateful to DESY for travel support.

229 **Conflicts of Interest:** The authors have declared that there are no conflicts of interests.

230 References

- 231 1. Shoji, E. Quinazoline Alkaloids and Related Chemistry. *Heterocycl Chem* **2006**, *6*, 113–156.
- 232 2. Shakhidoyatov, Kh. M.; Elmuradov, B. Zh. Tricyclic Quinazoline Alkaloids: Isolation, Synthesis, Chemical
233 Modification, and Biological Activity. *Chem Nat Compd* **2014**, *50*, 781–800.
- 234 3. Mashkovskiy, M. D. *Lekarstvennye Sredstva*, Tashkent, 1998.
- 235 4. Shakhidoyatov, Kh. M. *Khinazolony-4*. Ikh Biologicheskaya Aktivnost., FAN, Tashkent, 1988.
- 236 5. Al-Shamma, A.; Drake, S.; Flynn, D.L.; Mitscher, L.A.; Park, Y.H.; Rao, G.S.; Simpson, A.; Swayze, J.K.;
237 Veysoglu, T.; Wu, S.T. Antimicrobial agents from higher plants. Antimicrobial agents from Peganum
238 harmala seeds. *J. Nat Prod.* **1981**, *44(6)*, 745–747.
- 239 6. Tulyaganov, N. Pharmacological studies of alkaloids Peganum harmala L. quinazoline and quinazoline
240 structures and their derivatives. *Pharmacology of natural compounds*, **1979**, 71–80.
- 241 7. Fitzgerald, J. S.; Johns, S. R.; Lambertson, J. A.; Redcliffe, A. H. 6,7,8,9-Tetrahydropyridoquinazolines, a
242 new class of alkaloids from Mackinlaya species (Araliaceae). *Aust. J. Chem.* **1966**, *19(1)*, 151–159.
- 243 8. Elmuradov, B. Z.; Shakhidoyatov, K. M. Transformation of natural compounds. VII. Synthesis of
244 α -piperazinyl methylidene deoxyvasicinones. *Chem. Nat. Compd.* **1998**, *34(3)*, 298–299.
- 245 9. Elmuradov, B. Z., Chemical modifications of α -oxy-, -chloro-, -hydroselelylmethylidene-2,3-
246 trimethylene-3,4-dihydroquinazolin-4-ones, PhD dissertation, National University of Uzbekistan,
247 Tashkent, 2003.

- 248 10. Elmuradov, B.; Shakhidoyatov, Kh. M. Interaction of α -hydroxymethylidene-2,3-trimethylene-
249 3,4-dihydroquinazolin-4-one with amines. *Chem. Chem. Technol.* **2008**, *3*, 27-31.
- 250 11. Turdibayev, Z. E.; Elmuradov, B. Z.; Khakimov, M. M.; Shakhidoyatov, K. M.; Formylation of
251 deoxyvasicinone by alkylformates: synthesis and reaction of α -hydroxymethylidenedeoxyvasicinone with
252 isomeric aminophenols and aminobenzoic acids. *Chem. Nat. Compd.* **2011**, *47(4)*, 600-603.
- 253 12. Nasrullaev, A. O.; Turdibayev, Z. E.; Elmuradov, B. Z.; Yili, Abulimiti; Aisa, Haji Akber; Shakhidoyatov,
254 K. M. Chemical transformations of mackinazolinone and its derivatives. *Chem. Nat. Compd.* **2012**, *48(4)*, pp.
255 638-642.
- 256 13. Tojiboev, A.; Zhurakulov, Sh.; Vinogradova, V.; Englert, U.; Wang, R. Stereochemistry of the
257 methylidene-bridged quinazoline-isoquinoline alkaloid 3-[[6,7-dimethoxy-1-(4-nitrophenyl)-
258 -1,2,3,4-tetrahydroisoquinolin-2-yl]-methylidene]-1,2,3,9-tetrahydropyrrolo[2,1-b]-quinazolin-9-one
259 methanol monosolvate. *Acta Cryst. E* **2020**, *76*, 914-919.
- 260 14. Zhurakulov, Sh. N.; Vinogradova, V. I. Reaksiya 3-gidroksimetiliden-1,2,3,9-
261 tetragidropirrolo[2,1-b]-hinazolin-9-ona i 4-(formil)-1,2,3,4,10-pentagidropirido[2,1-b]-hinazolin-10-ona s
262 benzilaminom i psevdofedrinom. *Uzb. Chem. J.* **2015**, *5*, 25-29.
- 263 15. Zhurakulov, Sh. N.; Vinogradova, V. I. 3-Hydroxymethylidene-1,2,3,9-tetrahydropyrrolo[2,1-b]-
264 quinazolin-9-one and 4-(formyl)-1,2,3,4,10-pentahydropyrrolo[2,1-b]-quinazolin-10-one—new sintons for
265 obtaining of 3,4-dihydroisoquinolines. *Int. J. Chem. Phys. Sci.* **2016**, *5(1)*, 1-7.
- 266 16. Zhurakulov, Sh. N., Levkovich M. G.; Vinogradova V. I. Reactions of
267 3,4-Dimethoxyphenylethylaminomethylidene Derivatives Triand Tetramethylene-4-Quinazolones and
268 Formaldehyde. *Chem. Sustain. Dev.* **2017**, *25*, 265-269.
- 269 17. Sheldrick, G.M. A short history of SHELX. *Acta Cryst. Sect. A* **2008**, *64*, 112-122.
- 270 18. Sheldrick, G. M. Crystal structure refinement with SHELXL. *Acta Cryst. C* **2015**, *71*, 3-8.
- 271 19. McKinnon, J. J.; Jayatilaka, D.; Spackman, M. A. Towards quantitative analysis of intermolecular
272 interactions with Hirshfeld surfaces. *Chem Commun.* **2007**, 3814-3816.
- 273 20. Spackman, M. A.; Jayatilaka, D. Hirshfeld surface analysis. *CrystEngComm* **2009**, *11*, 19-32.
- 274 21. Mitchell, A.S. Novel tools for visualizing and exploring intermolecular interactions in molecular crystals.
275 *Acta Cryst. B* **2004**, *60*, 627-668.
- 276 22. Munshi, P.; Skelton, B.W.; McKinnon, J.J.; Spackman, M.A. Polymorphism in
277 3-methyl-4-methoxy-4'-nitrostilbene, a highly active NLO material. *CrystEngComm.* **2008**, *10*, 197-206.
- 278 23. Lemmerer, A.; Bernstein, J.; Spackman, M.A. Supramolecular polymorphism of the 1:1 molecular salt
279 (adamantane-1-carboxylate-3,5,7-tricarboxylic acid) (hexamethylenetetraminium). A "failed" crystal
280 engineering attempt. *Chem. Commun.* **2012**, *48*, 1883-1885.
- 281 24. Luo, Y.H.; Sun, B.W. Co-crystallization of pyridine-2-carboxamide with a series of alkyl dicarboxylic acids
282 with different carbon chain: crystal structure, spectroscopy and Hirshfeld analysis. *Spectrochim. Acta. A.*
283 **2014**, *120*, 228-236.
- 284 25. Nemkevich, A.; Spackman, M.A.; Corry, B. Simulations of Guest Transport in Clathrates of Dianins
285 Compound and Hydroquinone. *Chem. Eur. J.* **2013**, *19*, 2676-2684.
- 286 26. Lee, J.J.; Sobolev, A.N.; Turner, M.J.; Fuller, R.O.; Iversen, B.B.; Koutsantonis, G.A.; Spackman, M.A.
287 Molecular Imprisonment: Host Response to Guest Location, Orientation, and Dynamics in Clathrates of
288 Dianin's Compound. *Cryst. Growth Des.* **2014**, *14*, 1296-1306.
- 289 27. Grabowsky, S.; Dean, P.M.; Skelton, B.W.; Sobolev, A.N.; Spackman, M.A.; White, A.H. Crystal packing in
290 the 2-R,4-oxo-[1,3-a/b]-naphtho dioxanes – Hirshfeld surface analysis and melting point correlation.
291 *CrystEngComm.* **2012**, *14*, 1083-1093.
- 292 28. Spackman, M.A.; McKinnon, J.J. Fingerprinting intermolecular interactions in molecular crystals.
293 *CrystEngComm* **2002**, *4*, 378-392.
- 294 29. Turner, M.J.; McKinnon, J.J.; Wolff, S.K.; Grimwood, D.J.; Spackman, P.R.; Jayatilaka, D.; Spackman, M.A.
295 *CrystalExplorer17*; University of Western Australia: Pert, Australia, **2017**.
- 296 30. Spek, A. L. checkCIF validation ALERTS: what they mean and how to respond *Acta Cryst. E* **2020**, *76*, 1-11.
- 297 31. Mackenzie, C. F.; Spackman, P. R.; Jayatilaka, D.; Spackman, M. A. CrystalExplorer model energies and
298 energy frameworks: extension to metal coordination compounds, organic salts, solvates and open-shell
299 systems. *IUCrJ* **2017**, *4*, 575-587.
- 300



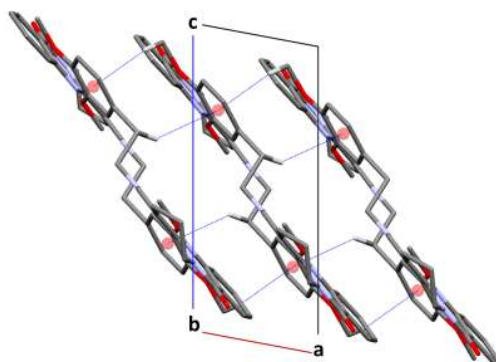
© 2020 by the authors. Submitted for possible open access publication under the terms and conditions of the Creative Commons Attribution (CC BY) license (<http://creativecommons.org/licenses/by/4.0/>).

301

302

303 **Supplementary Materials:**

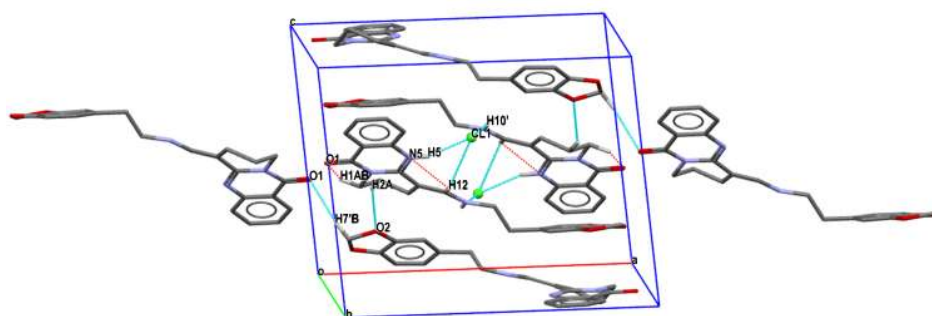
304



305

306 **Figure S1.** Layers are propagating parallel to (102) plane. H atoms not involved in interactions have
 307 been omitted for clarity.

308



309

310 **Figure S2.** Packing diagram for (2) with intramolecular C–H...O, C–H...N and intermolecular
 311 C–H...O, C–H...Cl, N–H...Cl hydrogen bonds shown, respectively, by red and blue dashed lines..
 312 H atoms not involved in hydrogen bonds have been omitted for clarity.

313

314

Table S1. Crystal data and structure refinement parameters for (1) and (2).

Compound	1	2
Chemical formula	C ₂₃ H ₂₅ N ₃ O ₃	C ₂₂ H ₂₂ N ₃ O ₃ ·Cl
<i>M_r</i>	391.46	411.87
Crystal system	Monoclinic	Monoclinic
Space group	<i>P</i> 2 ₁ / <i>c</i>	<i>P</i> 2 ₁ / <i>c</i>
Temperature (K)	100	100(2)
<i>a</i> (Å)	5.041(3)	15.005(10)
<i>b</i> (Å)	31.890(19)	10.425(7)
<i>c</i> (Å)	12.144(6)	12.186(9)
β (°)	100.60 (4)	95.671 (15)
Volume (Å ³)	1918.9 (19)	1897 (2)
<i>Z</i>	4	4
Radiation type	Synchrotron	Mo K α
Wavelength (Å)	0.560	0.710730

Absorption coefficient (mm ⁻¹)	0.06	0.23
Crystal size (mm)	0.05 × 0.02 × 0.01	0.13 × 0.12 × 0.01
F(000)	832	864
Absorption correction or scaling	Multi-scan, SADABS 2014/5	Multi-scan, TWINABS
<i>T</i> _{min} , <i>T</i> _{max}	0.692, 0.862	0.370, 0.862
<i>R</i> _{int}	0.182	0.082
No. of measured, independent and observed [<i>I</i> > 2σ(<i>I</i>)] reflections	39958, 4219, 2692	3457, 3457, 987
(sin θ/λ) _{max} (Å ⁻¹)	0.640	0.601
<i>R</i> [<i>F</i> ² > 2σ(<i>F</i> ²)]	0.115	0.091
<i>wR</i> (<i>F</i> ²)	0.249	0.169
Goodness-of-fit on <i>F</i> ²	1.19	0.090
No. of reflections	4219	3457
No. of parameters	307	262
No. of restraints	67	231
Δ <i>Q</i> _{max} , Δ <i>Q</i> _{min} (e Å ⁻³)	0.85, -0.42	0.44, -0.44

315

316

Table S2. Hydrogen-bond geometry (Å, °) for (1). Cg4 is the centroids of ring (C1'–C6').

<i>D</i> – <i>H</i> ⋯ <i>A</i>	<i>D</i> – <i>H</i>	<i>H</i> ⋯ <i>A</i>	<i>D</i> ⋯ <i>A</i>	<i>D</i> – <i>H</i> ⋯ <i>A</i>
N9B'–H9B'⋯N5	0.94(7)	2.03(7)	2.812(8)	139(8)
C1–H1AB⋯O1	0.99	2.31	2.708(6)	103
C6–H6⋯O2 ⁱ	0.95	2.59	3.506(7)	163
C12–H12B⋯O1 ⁱⁱ	0.95	2.43	3.374(10)	171
C7B'–H7BB⋯Cg4 ⁱⁱⁱ	0.99	2.88	3.665(11)	137
C11'–H11B⋯Cg4 ^{iv}	0.95	2.59	3.458(6)	147

317

Symmetry codes: (i) 1-x,1-y,1-z; (ii) 1+x,3/2-y,-1/2+z; (iii) -1+x,y,z; (iv) 1+x,y,z.

318

319

320

Table S3. Hydrogen-bond geometry (Å, °) for (2). Cg2 and Cg4 are the centroids of ring (N5/C4A/N11/C10/C9A/C5A) and (C1'–C6'), respectively.

<i>D</i> – <i>H</i> ⋯ <i>A</i>	<i>D</i> – <i>H</i>	<i>H</i> ⋯ <i>A</i>	<i>D</i> ⋯ <i>A</i>	<i>D</i> – <i>H</i> ⋯ <i>A</i>
N5–H5⋯C11	0.88	2.25	3.088(5)	159
N10'–H10'⋯C11 ⁱ	0.88	2.47	3.187(6)	139
C1–H1AB⋯O [`]	0.99	2.34	2.717(8)	101
C2–H2A⋯O2 ⁱⁱ	0.99	2.47	3.290(8)	140
C7'–H7'B⋯O1 ⁱⁱⁱ	0.99	2.41	3.397(8)	172
C12–H12⋯C11	0.95	2.77	3.342(7)	119
C12–H12⋯N5	0.95	2.46	2.797(8)	101
C2–H2AB⋯Cg4 ^{iv}	0.99	2.70	3.667(7)	165
C6'–H6'⋯Cg2 ⁱ	0.95	2.82	3.269(7)	110

321

Symmetry codes: (i) 1-x,1-y,1-z; (ii) 1-x,-1/2+y,3/2-z; (iii) -1+x,3/2-y,1/2+z.

322